Biochemical and Biophysical Research Communications 438 (2013) 715–720

Contents lists available at ScienceDirect

Biochemical and Biophysical Research Communications

journal homepage: www.elsevier.com/locate/ybbrc

Characterization and comparative analysis of psychrophilic and mesophilic alpha-amylases from *Euplotes* species: A contribution to the understanding of enzyme thermal adaptation

Guang Yang [1], Guang Yang [2], Lino Aprile, Vincenzo Turturo, Sandra Pucciarelli, Stefania Pucciarelli, Cristina Miceli *

School of Biosciences and Biotechnology, University of Camerino, Italy

ARTICLE INFO

Article history:
Received 19 July 2013
Available online 2 August 2013

Keywords:
Molecular cold adaptation
Molecular interactions
Psychrophilic enzymes
Biochemical activity

ABSTRACT

The eukaryotic α-amylase isolated from the psychrophilic ciliated protozoon *Euplotes focardii* (*Ef*Amy) was expressed in *Escherichia coli* and biochemically characterized. Its enzymatic activity was compared to that of the homologous protein from the mesophilic congeneric species *Euplotes crassus* (*Ec*Amy). The comparison of the amino acid composition and the surface residue composition of the two enzymes indicated a preference for tiny residues and the avoidance of charged, aromatic and hydrophobic residues in *Ef*Amy. Our comparative homology modeling study reveals a lack of surface salt bridges, a decreased number of the surface charged residues, decreased hydrogen bonds and bound ions, and a reduction of aromatic-sulfur interactions, cationic–π interactions and disulfide interactions in *Ef*Amy. In contrast, sequence alignment and homology modeling showed five unconserved prolines located on the surface loops of *Ec*Amy. By analyzing amylolytic activity towards soluble starch as the substrate, we determined the temperature and pH dependence, thermostability and kinetic parameters of these two enzymes. We demonstrated that *Ef*Amy shows the characteristics of a psychrophilic α-amylase, such as the highest hydrolytic activity at low temperatures and high thermolability. In contrast, the *Ec*Amy showed mesophilic characteristics with the highest activity at moderate temperatures and a more than 2-fold increased half-life at 50 °C compared to *Ef*Amy. The k_{cat} and K_M values of *Ef*Amy were higher than those of the mesophilic *Ec*Amy at all tested temperatures. Furthermore, both *Ef*Amy and *Ec*Amy showed maximum activities at pH 9 and maintained high activities in the presence of surfactants. These results suggest the potential applications of *Ef*Amy and *Ec*Amy as ingredients in detergents for industrial applications.

1. Introduction

α-Amylases (EC 3.2.1.1) are hydrolases that randomly cleave the 1,4-α-D-glucosidic linkages between adjacent glucose units in the linear amylose chain of starch, yielding as final products maltotriose or maltose [1–3]. Amylases are among the most important industrial enzymes and are of great significance for biotechnology, constituting a class of that represents approximately 30% of the world's industrial enzyme production [4]. Due to the widespread use of amylases in a variety of industrial applications, it would be beneficial to identify enzymes that possess high catalytic efficiency with reduced energy costs. Cold-active enzymes produced by psychrophilic organisms possess high specific activities at low temperatures in comparison to the enzymes from mesophiles or thermopiles, which normally show little or no activity at low temperatures [5]. In addition, cold-active enzymes usually show relatively high thermosensitivity, providing the possibility to rapidly inactivate these enzymes in complex applications [6]. Therefore, cold-active α-amylases have emerged as ideal biocatalysts, having broad potential in industrial applications [7]. The production of thermophilic α-amylases by various bacteria and fungi has been well documented [8,9]. In contrast, less attention has been paid to cold-active α-amylases from psychrophiles [10], in particular from psychrophilic eukaryotic unicellular organisms.

The ciliated protozoon *Euplotes focardii*, originally isolated from the coastal seawaters of Terra Nova Bay in Antarctica, shows strictly psychrophilic phenotypes: its optimal temperature of survival and reproduction is 4–5 °C; it lacks a transcriptional response of the *Hsp70* genes to thermal shock [11]; and it possesses cold-stable microtubules [12,13], cold-active phospholipases [14] and modified ribosomal proteins [15]. In the present study, we report

* Corresponding author. Address: School of Biosciences and Biotechnology, University of Camerino, Via Gentile III da Varano, 62032 Camerino, MC, Italy. Fax: +39 0737 40 32 90.
E-mail address: cristina.miceli@unicam.it (C. Miceli).
[1] Postdoctoral Fellow.
[2] Master Student.

0006-291X/$ - see front matter © 2013 Elsevier Inc. All rights reserved.
http://dx.doi.org/10.1016/j.bbrc.2013.07.113

the first comprehensive study of the purification and characterization of an efficient psychrophilic eukaryotic α-amylase from *E. focardii* (named *Ef*Amy). In addition, we purified and characterized a homologous enzyme from the evolutionarily close mesophilic species *Euplotes crassus* (*Ec*Amy). The catalytic properties of both enzymes are compared and reported.

2. Materials and methods

2.1. Cell strains and growth conditions

Cultures of *E. focardii* strain TN1 [16] and *E. crassus* strain G1 were used. *E. focardii* strain TN1 was grown and maintained in a cold room at 4 °C. The mesophilic *E. crassus* strain G1 was kindly obtained from the strain collection of Luporini's laboratory at the University of Camerino. *Escherichia coli* DH5α was used as a host for cloning, whereas *E. coli* BL21 (DE3) pLysS was used for gene expression. *E. coli* strains were routinely grown in LB medium at 37 °C. When required, antibiotics were added at the following concentrations: 100 μg/ml ampicillin and 34 μg/ml chloramphenicol.

2.2. Isolation of Euplotes amylase nanochromosomes

E. focardii macronuclear DNA was purified as described [17]. To obtain the primary partial *Ef*Amy sequence, we based our PCR strategy on degenerate oligonucleotide primers designed against the *Euplotes* α-amylase consensus sequence (obtained by the alignment of homologous genes from *E. crassus*, which were kindly provided by the laboratory of Professor Gladyshev, Harvard Medical School, USA). Degenerate oligonucleotide primers were designed according to the improved CODEHOP primer design method [18]. The forward primer, 5'-TATGTGGHTMATGVTCGATGTWGT 0TGCTAATCA-3', covered codons 124–133 plus two nucleotides from codon 134, and the reverse primer, 5'-TMGCRWTATCVTGGT-TAATCADCAAAAGTTCC-3', corresponded to one nucleotide of codon 304 plus triplets 294–303.

Based on the organization of nanochromosomes in *Euplotes* spp. [19], RATE (Rapid Amplification of Telomere Ends) PCR [17] was performed for obtaining the sequences of N-terminal and C-terminal coding regions and the 5'- and 3'-UTRs. The forward primer, 5'-TGATGGTCTTAGAATCGACACTGTA-3', and the reverse primer, 5'-TACAGTGTCGATTCTAAGACCATCA-3', were individually used in combination with the telomeric oligonucleotide 5'-$(C_4A_4)_4$-3' in RATE PCR. Amplified products were cloned into pTZ57R/T vector (Fermentas, Milan, Italy) to construct the plasmid pTZ57R/T-*Ef*Amy and then transformed into *E. coli* DH5α. Clones containing the *Ef*Amy recombinant plasmids were sequenced in both strands (BMR Genomics, Padova, Italy).

The *Ef*Amy gene was amplified again from the previous constructed plasmid pTZ57R/T-*Ef*Amy, while the *Ec*Amy gene was amplified from *E. crassus* genomic DNA. Oligonucleotides *Ef*NdeI (5'-CATATGGCTCACAGCACAGAAGAATGGA-3'), *Ef*XhoI (5'- CTCGAG TTCACTCACTGTTGCAGTCT-3') were used as forward and reverse primers for amplification of *Ef*Amy. *Ec*NdeI (5'-CTAATGGCT CATAAC ACTGAGGAATGGA-3') and *Ec*XhoI (5'-CTCGAGTTCCTTAATAAGTC TGGCCT-3') were used as forward and reverse primers for amplification of *Ec*Amy. The amplification primers *Ef*NdeI, *Ef*XhoI and *Ec*NdeI, *Ec*XhoI were designed to introduce NdeI restriction sites upstream from the initiation sites and XhoI restriction sites downstream from the stop codons of *Ef*Amy and *Ec*Amy, respectively. The PCR products were ligated into the pTZ57R/T vector and then transformed into *E. coli* DH5α, and clones containing *Ef*Amy and *Ec*Amy recombinant plasmids were sequenced in both strands (BMR Genomics, Padova, Italy). The complete *Euplotes* α-amylase sequences are available on GeneBank™ by accession numbers: KF421593 (*Ef*Amy) and KF421594 (*Ec*Amy).

2.3. Construction of pET22b-EfAmy and pET22b-EcAmy

The *Ef*Amy and *Ec*Amy recombinant plasmids were digested by NdeI and XhoI restriction enzymes (Fermentas, Milan, Italy), resulting in the removal of predicted signal peptides of the proteins. Both proteins were cloned into the pET-22b(+) expression vector that was previously digested by NdeI and XhoI restriction enzymes to obtain the pET22b-*Ef*Amy and pET22b-*Ec*Amy expression plasmids. The DNA sequences of the resulting constructs were verified by bidirectional DNA sequencing.

2.4. Overexpression and purification of Euplotes α-amylases

E. coli BL21 (DE3)pLysS cells carrying *Euplotes* α-amylase plasmids were grown overnight at 37 °C in LB medium supplemented with 100 μg/ml ampicillin and 34 μg/ml chloramphenicol. The overnight cultures were diluted to a cell density of about OD_{600} 0.08 in 600 ml of LB medium supplemented with 100 μg/ml ampicillin and 34 μg/ml chloramphenicol in a 2-L flask. Cultivation was conducted at 30 °C with vigorous stirring and aeration. The induction procedures were carried out when cultures reached OD_{600} of 0.6–0.8 by the addition of IPTG to a final concentration of 0.1 mM. The cultures were grown overnight for post-induction. Cells were harvested by centrifugation at 5000*g* at 4 °C for 20 min, divided into 0.50-g aliquots and frozen at −80 °C.

The IPTG induction of recombinant *E. coli* BL21 (DE3) pLysS cells resulted in the accumulation of recombinant *Euplotes* α-amylases as inclusion bodies. The recovery procedure was conducted following a previous description for the purification of *E. focardii* patatin-like phospholipase [14].

2.5. Protein analysis

SDS–PAGE on 12% polyacrylamide was performed by the method of Laemmli [20]. Native 12% PAGE was also performed as described in the Bio-Rad instruction manual. After electrophoresis, the native polyacrylamide gel was soaked for 30 min in 1% soluble starch in 0.1 M Tris–HCl buffer (pH 9) at room temperature with slow shaking. Amylase bands were visualized by staining the gel with KI–I_2 solution (0.5% KI and 0.05% I_2). The protein concentration was determined according to the Bradford method with bovine serum albumin as the standard [21].

2.6. Enzyme assays

The α-amylase enzyme activity was measured according to the modified method of Xiao et al. [22]. Briefly, the reaction was performed by adding 0.1 ml of starch solution (2 g/l) as a substrate to the enzyme solution containing 0.1 ml of enzyme (0.4 mg/ml) in 0.1 M Tris–HCl buffer (pH 9). The reaction mixture was incubated for 20 min at 25 and 35 °C for *Ef*Amy and *Ec*Amy, respectively, at which temperatures the assayed enzymes were most active. The α-amylase activity was confirmed by adding 0.1 ml of iodine reagent (0.5% KI and 0.05% I_2) to 0.2 ml of the protein–starch solution. Following color development, the formation of a starch–iodine complex was monitored on the spectrophotometer at 580 nm (A_{580}). A unit of α-amylase activity was defined in terms of the amount of enzyme that released 1 mg reducing sugar per minute under the mentioned conditions.

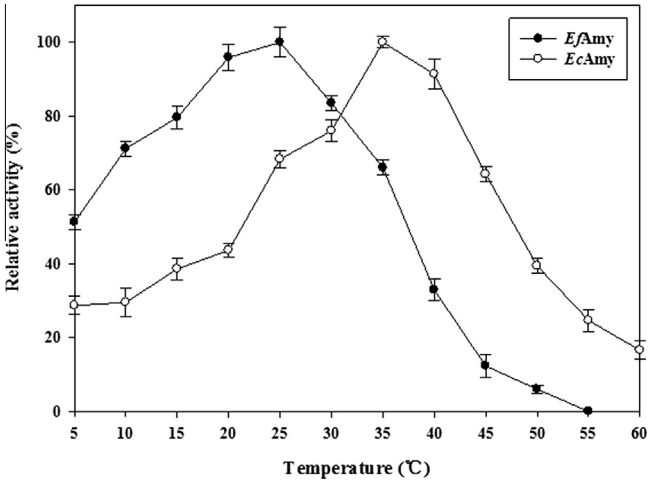

Fig. 1. Effect of temperature on the amylolytic activity of *Ef*Amy and *Ec*Amy.

2.7. Effect of pH and temperature on enzyme activity and stability

The optimal pHs of the *Euplotes* α-amylases were determined by incubating the assay reaction mixture in the following buffers (all at a concentration of 0.1 M): MES (pH 5.0–7.0), Tris–HCl (pH 7.0–9.0) and glycine–NaOH (pH 9.0–11.0).

The optimal temperatures for the *Euplotes* α-amylases were determined by incubating the reaction mixture in the range of temperature from 0 to 60 °C in 0.1 M Tris–HCl buffer (pH 9).

The half-lives of thermal inactivation were determined for purified α-amylases by incubating the enzymes in 0.1 M Tris–HCl buffer (pH 9) at 40 and 50 °C for 0–20 min with regular time intervals. Initial and residual activities were measured under the standard assay conditions previously described. The first-order rate constant, k_d, of irreversible thermal denaturation was obtained from the slope of the plots of ln(initial activity/residual activity) versus time, and the half-lives ($t_{1/2}$) were calculated as $\ln 2/k_d$.

2.8. Kinetic measurements

The kinetic parameters, K_M and k_{cat}, of *Ef*Amy and *Ec*Amy were measured using soluble starch as the substrate at 5, 25 and 35 °C. The substrate concentration range used was 0.5 to 8 g/l. All kinetic data were analyzed by nonlinear regression using Origin 8.0. The Standard Error (S.E.) of each parameter was estimated from the curve fitting.

2.9. Sequence analysis and comparative modeling

Sequence alignments were performed using ClustalW2 (http://www.ebi.ac.uk/Tools/msa/clustalw2/). The N-terminal signal peptides were predicted using the SignalP 4.1 server (http://www.cbs.dtu.dk/services/SignalP/). The comparative homology models of the *Euplotes* α-amylases were obtained by the program SWISS-MODEL [23], with the Taka α-amylase A (TAA) from *Aspergillus oryzae* (PDB: 2TAA) as a specific template. The amino acid sequences of *Euplotes* α-amylases and TAA shared 34% and 36% identities for *Ef*Amy and *Ec*Amy, respectively (Fig. S1B). Protein interactions were calculated using Protein Interactions Calculator [24]. Protein surface residues were predicted with NetSurfP [25].

3. Results

3.1. Cloning, expression and purification of Euplotes α-amylases

With a RATE-PCR-based cloning strategy (see Section 2), we obtained the entire sequences of the α-amylase nanochromosome from *E. focardii* (schematically represented in Fig. S1A) and *E. crassus*. The coding regions were 1395 and 1404 bp long, respectively. The predicted amino acid sequences of both *Ef*Amy and *Ec*Amy show similarity to the conserved regions of α-amylase characterized in previous studies (Fig. S1A and B) [26,27], confirming that both enzymes are α-amylases.

The coding regions of both *Ef*Amy and *Ec*Amy were subcloned into the pET22b(+) vector, expressed in *E. coli* BL21 (DE3) pLysS cells, and purified from inclusion bodies, as described in Section 2. As estimated from SDS–PAGE (Fig. S2A), the sizes of recombinant refolded *Ef*Amy and *Ec*Amy were 52 kDa and 53 kDa, respectively, and they were approximately 95% pure. The activity staining of a native 12% PAGE gel (performed as described under Section 2) showed the presence of two bands with similar migrating properties (Fig. 2B).

3.2. Euplotes α-amylases' optimal pH, thermophilicity, thermostability and kinetic parameters

The pH-dependence assays indicated that both *Ef*Amy and *Ec*Amy reached the highest activities at pH 9 in 0.1 M Tris–HCl (Fig. S3).

Under the standard conditions used, *Ef*Amy showed the highest activity at approximately 20–25 °C (Fig. 1). Fifty percentof maximal activity was observed at 0 °C, and approximately 10% residual activity remained at 45 °C. In contrast, *Ec*Amy showed low activity at 5–15 °C, reached its maximum activity at 35 °C and maintained approximately 20% maximal activity at 60 °C.

To analyze the thermostability of *Euplotes* α-amylases, we incubated both *Ef*Amy and *Ec*Amy at 40 and 50 °C for 2–20 min before measuring the residual activities at their optimal temperatures (Fig. 2). As shown in Table 1, *Ec*Amy showed 6.5 and 4.2 min half-lives at 40 and 50 °C, respectively, whereas the psychrophilic counterpart *Ef*Amy displayed lower stability at the same temperatures with 4.1 and 1.8 min half-lives.

The results of kinetic study showed an increased turnover rate (increase in k_{cat}) and decreased substrate binding affinity of *Ef*Amy (increase in K_M) at 5, 25 and 35 °C (Table 2) when compared to *Ec*Amy. A comparison of the k_{cat}/K_M ratio indicates that *Ec*Amy possessed higher catalytic efficiency at all temperatures, with the most significant increase at 35 °C, at which temperature *Ec*Amy had 3-fold higher catalytic efficiency than that of *Ef*Amy.

3.3. Sequence and structural model analysis of Euplotes α-amylases

*Ef*Amy and *Ec*Amy shared 68% identity in amino acid sequences (Fig. S1B). However, these two enzymes showed significantly

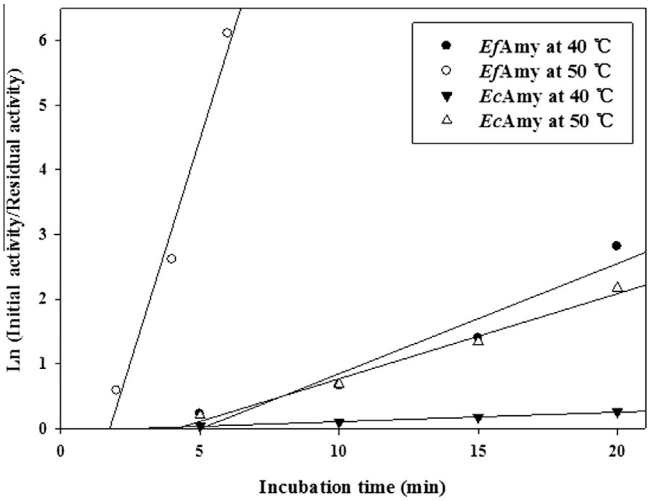

Fig. 2. Thermostability of *Ef*Amy (● and ○) and *Ec*Amy (▼ and △) at 40 °C (● and ▼) and 50 °C (○ and △).

Table 1
Stability properties (half-lives) of *Ef*Amy and *Ec*Amy at 40 and 50 °C.

Enzyme	$t_{1/2}$ (40 °C, min)	$t_{1/2}$ (50 °C, min)	T_{opt} (°C)
*Ef*Amy	4.1 ± 0.13	1.8 ± 0.11	25
*Ec*Amy	6.5 ± 0.27	4.2 ± 0.16	35

different catalytic properties, especially in temperature dependences and thermostabilities. We therefore compared the amino acid composition and the surface residues of the two enzymes to look for potential elements that may affect thermal-adaptation (Table S2). *Ef*Amy and *Ec*Amy differed primarily in three aspects: (i) *Ef*Amy contained a higher overall percentage of tiny residues (Ala, Cys, Gly, Ser and Thr) than *Ec*Amy (24.5% versus 21.4%, respectively) and a higher percentage of tiny surface residues (29.8% versus 24.5%, respectively); (ii) *Ef*Amy contained less charged residues than *Ec*Amy at both the total and the surface levels (2.5% and 4.1%, respectively); (iii) *Ef*Amy contained 2.5% and 2.1% less aromatic and hydrophobic surface residues, respectively, when compared to *Ec*Amy (8.5% versus 10.9% for aromatic residues and 17.4% versus 19.5% for hydrophobic residues). Other remarkable factors are that *Ec*Amy contained a higher number of prolines (20) than *Ef*Amy (15), and *Ec*Amy had two more unconserved cysteines in domain C (Fig. 3 and Fig. S1B).

The structural models of *Euplotes* α-amylases were analyzed to compare the interactions and the structural features for further identification of the potential parameters involved in the structural flexibility of *Ef*Amy. As shown in Table 3, the number of ionic interactions and electrostatic forces is lower in *Ef*Amy. These characteristics may be a consequence of the cold-adaptation of *E. focardii*, because they may confer an increased structural flexibility. In contrast, the strong conservation of aromatic–aromatic and hydrophobic interactions certainly reflects their essential function in the conformation of both enzymes.

Table 3
Structural parameters potentially involved in the stability of α-amylase conformation.

Parameters	*Ef*Amy (T_{opt} 25 °C)	*Ec*Amy (T_{opt} 35 °C)
Electrostatic forces	255	282
Ionic interactions	57	102
Salt bridges	28	43
Hydrophobic interactions	52	52
Aromatic–aromatic interactions	32	34
Aromatic–sulfur interactions	5	8
Cationic–π interactions	8	10
Disulfide interactions	2	3
Net charges	−32	−40
Proline contents	15	20

4. Discussion

This study reports the recombinant production, purification and biochemical characterization of cold-active *Ef*Amy produced by the psychrophilic ciliate *E. focardii*. In addition, a homologous enzyme from mesophilic *E. crassus* was expressed and characterized to perform a comparative study. Both proteins were recovered in a homogeneous form. The activity staining of a native gel confirmed the high purity and activity for both enzymes (Fig. S2A and B). Biochemical assays indicated that both *Ef*Amy and *Ec*Amy reached maximum activity at pH 9, which is in line with the amylases from the marine bacteria *Halobacterium salinarum* [28] and *Streptomyces* sp. [29]. This biochemical characteristic, together with the findings that we obtained on the effects of surfactants (EDTA, SDS and Triton X100) on enzyme activities (Table S1), suggests the potential application of *Euplotes* α-amylases as ingredients in detergents for automatic dishwashers and clothes washers for the hydrolysis of starch under moderate to high pH conditions.

Table 2
Kinetic parameters of *Ef*Amy and *Ec*Amy at 5, 25, and 35 °C.

Enzyme	Temperature (°C)	k_{cat} (s^{-1})	K_M (g l^{-1})	k_{cat}/K_M (s^{-1} g^{-1} l)
*Ef*Amy	5	718.55 ± 31.91	3.05 ± 0.08	235.59 ± 16.65
	25	1466.42 ± 46.12	3.31 ± 0.16	443.03 ± 35.43
	35	982.51 ± 33.18	4.43 ± 0.19	221.78 ± 17.03
*Ec*Amy	5	377.53 ± 19.33	1.31 ± 0.04	288.19 ± 23.58
	25	618.91 ± 23.92	1.36 ± 0.03	455.08 ± 27.64
	35	879.76 ± 27.61	1.42 ± 0.07	619.55 ± 50.11

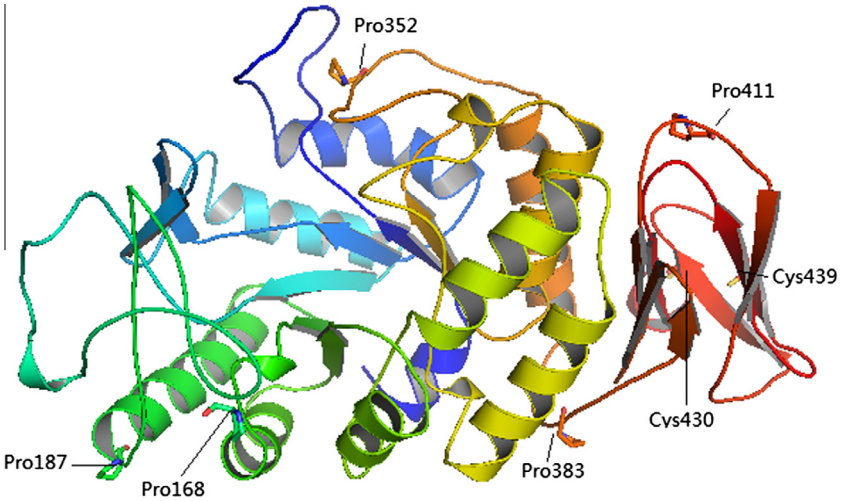

Fig. 3. Low-resolution homology model of *Ec*Amy. Unconserved residues are labeled with numbers.

The thermal dependence and stability studies demonstrated that *Ef*Amy behaves as a classical psychrophilic enzyme, because it is characterized by the highest activity at low temperatures and high thermolability. Considering that cold-active enzymes usually maintain a high structural flexibility generally accompanied by a trade-off of heat lability [30], we can hypothesize that the thermolability of *Ef*Amy may reflect a higher flexibility of its protein structure. In contrast, *Ec*Amy shows mesophilic characteristics, because the highest hydrolytic activity is achieved at moderate temperatures, and its half-life at 50 °C is more than 2-fold higher than that of *Ef*Amy.

The k_{cat} and K_M values of cold-active *Ef*Amy are higher than those of the mesophilic *Ec*Amy at all tested temperatures. This result is comparable with the previous research reported by Feller et al. [31], in which a cold active α-amylase (AHA) from the Antarctic psychrophile bacterium *Alteromonas haloplanctis* was compared with the mesophilic porcine homolog. In contrast, the relatively rapid increase in K_M and the decrease in the k_{cat}/K_M values of *Ef*Amy in the temperature range of 25–35 °C (Table 2) imply a susceptibility for the *Ef*Amy protein structure to be unfolded at these temperatures.

The analysis of the structural models of *Euplotes* α-amylases has indicated several parameters that can potentially contribute to the increased structural flexibility of *Ef*Amy, supporting the differences of catalytic properties discussed above. As shown in Table 3, the *Ef*Amy model is characterized by the lack of 15 surface salt bridges, when compared to *Ec*Amy. The lack of salt bridges in *Ef*Amy was primarily due to the decreased amount of charged residues overall and at the surface. It has been verified that the optimization of the surface charges is a promising strategy for increasing the thermostability of proteins [32]. Indeed, the changes at the protein surface rather than the decreased numbers of salt bridges resulted in greater entropic effects to the structure. A recent report on the temperature-dependent activity of proteins has pointed to the decreasing numbers of hydrogen bonds and bound ions at the surface [33]. This is in accordance with our finding that *Ef*Amy possesses less aromatic and hydrophobic residues at the surface, also considering that aromatic-sulfur interactions, cationic–π interactions and disulfide interactions are among the most important factors that contribute to protein structural stability. All of these elements were observed to be decreased in *Ef*Amy.

It is also interesting to note that fiveunconserved proline residues were detected by the sequence alignment of *Ef*Amy and *Ec*Amy (Fig. S1B). From the structural model study, we observed that these unconserved proline residues were located on the surface loops of *Ec*Amy (Fig. 3). Since the pyrrolidine ring of proline has endowed the residue a more rigid conformation, these residues usually reduce the flexibility of the protein structure. In addition, we observed two unconserved cysteines (Cys411 and Cys439) in the C-terminal domain of *Ec*Amy (Fig. 3 and Fig. S1B), where they most likely form a disulfide bond. However, a previous analysis reported that the deletion of the C-terminal region of the α-amylase from *Bacillus* sp. did not affect thermal stability and activity [34]. Therefore, the role of unconserved cysteines in the C-terminal domain of *Ec*Amy still needs to be clarified.

In conclusion, our results suggest that *Ef*Amy has evolved characteristics to increase its structural flexibility to improve catalytic activity at low temperatures. Therefore, our cold-active α-amylase emerges as a potential biocatalyst for industrial applications with low energy cost. In the past few decades, the production of maltodextrin, modified starches, or glucose and fructose syrups from starch, the major storage product of many economically important crops, has been based on enzymatic reactions rather than acid hydrolysis [4]. Starch-converting enzymes are also being used in a number of other industrial applications, such as laundry and porcelain detergents or as anti-staling agents in baking. Currently, these enzymes comprise approximately 30% of the world's enzyme production. The characterization of the alpha-amylase from *E. focardii* not only contributes to the comprehension of the molecular mechanisms responsible for enzyme cold-adaptation but also provides a new tool for these industrial processes.

Acknowledgments

We sincerely thank Dr. Donatella de Pascale (Institute of Protein Biochemistry, CNR, Naples) for helpful discussion. This research was supported by grants from the Italian "Programma Nazionale di Ricerche in Antartide" (PNRA) and from the Italian "Ministero dell'Istruzione, dell'Università e della Ricerca" (MIUR) (PRIN 2008) to CM. We acknowledge the COST (action BM1102) for supporting part of this work.

Appendix A. Supplementary data

Supplementary data associated with this article can be found, in the online version, at http://dx.doi.org/10.1016/j.bbrc.2013.07.113.

References

[1] A. Pandey, P. Nigam, C.R. Soccol, V.T. Soccol, D. Singh, R. Mohan, Advances in microbial amylases, Biotechnol. Appl. Biochem. 31 (Pt 2) (2000) 135–152.
[2] R. Gupta, P. Gigras, H. Mohapatra, V.K. Goswami, B. Chauhan, Microbial alpha-amylases: a biotechnological perspective, Process Biochem. 38 (2003) 1599–1616.
[3] L. Kandra, α-Amylases of medical and industrial importance, J. Mol. Struct. (Thoechem) 666–667 (2003) 487–498.
[4] M.J. van der Maarel, B. van der Veen, J.C. Uitdehaag, H. Leemhuis, L. Dijkhuizen, Properties and applications of starch-converting enzymes of the alpha-amylase family, J. Biotechnol. 94 (2002) 137–155.
[5] S. D'Amico, T. Collins, J.C. Marx, G. Feller, C. Gerday, Psychrophilic microorganisms: challenges for life, EMBO Rep. 7 (2006) 385–389.
[6] J.C. Marx, T. Collins, S. D'Amico, G. Feller, C. Gerday, Cold-adapted enzymes from marine Antarctic microorganisms, Mar. Biotechnol. (NY) 9 (2007) 293–304.
[7] A. Méndez-Vilas, Current Research, Technology and Education Topics in Applied Microbiology and Microbial Biotechnology, Formatex Research Center, Badajoz, Spain, 2010.
[8] B. Arikan, Highly thermostable, thermophilic, alkaline, SDS and chelator resistant amylase from a thermophilic Bacillus sp. isolate A3-15, Bioresour. Technol. 99 (2008) 3071–3076.
[9] A.C. Aquino, J.A. Jorge, H.F. Terenzi, M.L. Polizeli, Studies on a thermostable alpha-amylase from the thermophilic fungus *Scytalidium thermophilum*, Appl. Microbiol. Biotechnol. 61 (2003) 323–328.
[10] N. Samie, K.A. Noghabi, Z. Gharegozloo, H.S. Zahiri, G. Ahmadian, H. Sharafi, R. Behrozi, H. Vali, Psychrophilic alpha-amylase from *Aeromonas veronii* NS07 isolated from farm soils, Process Biochem. 47 (2012) 1381–1387.
[11] A. La Terza, C. Miceli, P. Luporini, The gene for the heat-shock protein 70 of Euplotes focardii, an Antarctic psychrophilic ciliate, Antarctic Science 16 (2004) 23–28.
[12] F. Chiappori, S. Pucciarelli, I. Merelli, P. Ballarini, C. Miceli, L. Milanesi, Structural thermal adaptation of beta-tubulins from the Antarctic psychrophilic protozoan *Euplotes focardii*, Proteins Struct. Funct. Bioinform. 80 (2012) 1154–1166.
[13] S. Pucciarelli, A. La Terza, P. Ballarini, S. Barchetta, T. Yu, F. Marziale, V. Passini, B. Methe, H.W. Detrich 3rd, C. Miceli, Molecular cold-adaptation of protein function and gene regulation: the case for comparative genomic analyses in marine ciliated protozoa, Mar. Genomics 2 (2009) 57–66.
[14] G. Yang, C. De Santi, D. de Pascale, S. Pucciarelli, S. Pucciarelli, C. Miceli, Characterization of the first eukaryotic cold-adapted patatin-like phospholipase from the psychrophilic *Euplotes focardii*: identification of putative determinants of thermal-adaptation by comparison with the homologous protein from the mesophilic *Euplotes crassus*, Biochimie (2013). http://dx.doi.org/10.1016/j.biochi.2013.06.008.
[15] S. Pucciarelli, F. Marziale, G. Di Giuseppe, S. Barchetta, C. Miceli, Ribosomal cold-adaptation: characterization of the genes encoding the acidic ribosomal P0 and P2 proteins from the Antarctic ciliate *Euplotes focardii*, Gene 360 (2005) 103–110.
[16] A. Valbonesi, P. Luporini, Description of two new species of *Euplotes* and *Euplotes rariseta* from Antarctica, Polar Biol. 11 (1990) 47–53.
[17] S. Pucciarelli, C. Miceli, Characterization of the cold-adapted alpha-tubulin from the psychrophilic ciliate *Euplotes focardii*, Extremophiles 6 (2002) 385–389.
[18] T.M. Rose, E.R. Schultz, J.G. Henikoff, S. Pietrokovski, C.M. McCallum, S. Henikoff, Consensus-degenerate hybrid oligonucleotide primers for

amplification of distantly related sequences, Nucleic Acids Res. 26 (1998) 1628–1635.
[19] D.C. Hoffman, R.C. Anderson, M.L. Dubois, D.M. Prescott, Macronuclear gene-sized molecules of hypotrichs, Nucleic Acids Res. 23 (1995) 1279–1283.
[20] U.K. Laemmli, Cleavage of structural proteins during the assembly of the head of bacteriophage T4, Nature 227 (1970) 680–685.
[21] N.J. Kruger, The Bradford method for protein quantitation, Methods Mol. Biol. 32 (1994) 9–15.
[22] Z. Xiao, R. Storms, A. Tsang, A quantitative starch-iodine method for measuring alpha-amylase and glucoamylase activities, Anal. Biochem. 351 (2006) 146–148.
[23] L. Bordoli, F. Kiefer, K. Arnold, P. Benkert, J. Battey, T. Schwede, Protein structure homology modeling using SWISS-MODEL workspace, Nat. Protoc. 4 (2009) 1–13.
[24] K.G. Tina, R. Bhadra, N. Srinivasan, PIC: protein interactions calculator, Nucleic Acids Res. 35 (2007) W473–476.
[25] B. Petersen, T.N. Petersen, P. Andersen, M. Nielsen, C. Lundegaard, A generic method for assignment of reliability scores applied to solvent accessibility predictions, BMC Struct. Biol. 9 (2009) 51.
[26] R. Nakajima, T. Imanaka, S. Aiba, Comparison of amino acid sequences of eleven different α-amylases, Appl. Microbiol. Biotechnol. 23 (1986) 355–360.
[27] M. Machius, G. Wiegand, R. Huber, Crystal structure of calcium-depleted *Bacillus licheniformis* alpha-amylase at 2.2 Å resolution, J. Mol. Biol. 246 (1995) 545–559.
[28] S. Shanmughapriya, G.S. Kiran, J. Selvin, R. Gandhimathi, T.B. Baskar, A. Manilal, S. Sujith, Optimization, production, and partial characterization of an alkalophilic amylase produced by sponge associated marine bacterium *Halobacterium salinarum* MMD047, Biotechnol. Bioprocess Eng. 14 (2009) (2009). 871-871 (vol 14, pg 67, 2009).
[29] S. Chakraborty, A. Khopade, C. Kokare, K. Mahadik, B. Chopade, Isolation and characterization of novel α-amylase from marine *Streptomyces* sp. D1, J. Mol. Catal. B Enzym. 58 (2009) 17–23.
[30] K.S. Siddiqui, R. Cavicchioli, Cold-adapted enzymes, Annu. Rev. Biochem. 75 (2006) 403–433.
[31] G. Feller, F. Payan, F. Theys, M. Qian, R. Haser, C. Gerday, Stability and structural analysis of alpha-amylase from the Antarctic psychrophile *Alteromonas haloplanctis* A23, Eur. J. Biochem. 222 (1994) 441–447.
[32] K.L. Schweiker, G.I. Makhatadze, A computational approach for the rational design of stable proteins and enzymes: optimization of surface charge–charge interactions, Methods Enzymol. 454 (2009) 175–211.
[33] G. Feller, Protein stability and enzyme activity at extreme biological temperatures, J. Phys. Condens. Matter. 22 (2010).
[34] H.F. Lo, L.L. Lin, W.Y. Chiang, M.C. Chie, W.H. Hsu, C.T. Chang, Deletion analysis of the C-terminal region of the alpha-amylase of *Bacillus* sp. strain TS-23, Arch. Microbiol. 178 (2002) 115–123.